AIP | Review of Scientific Instruments

Scanning droplet cell for high throughput electrochemical and photoelectrochemical measurements

John M. Gregoire, Chengxiang Xiang, Xiaonao Liu, Martin Marcin, and Jian Jin

Citation: Rev. Sci. Instrum. **84**, 024102 (2013); doi: 10.1063/1.4790419
View online: http://dx.doi.org/10.1063/1.4790419
View Table of Contents: http://rsi.aip.org/resource/1/RSINAK/v84/i2
Published by the American Institute of Physics.

Scanning droplet cell for high throughput electrochemical and photoelectrochemical measurements

John M. Gregoire,[1,a)] Chengxiang Xiang,[1] Xiaonao Liu,[1] Martin Marcin,[1] and Jian Jin[1,2]
[1]*Joint Center for Artificial Photosynthesis, California Institute of Technology, Pasadena, California 91125, USA*
[2]*Engineering Division, Lawrence Berkeley National Laboratory, Berkeley, California 94720, USA*

(Received 15 October 2012; accepted 22 January 2013; published online 12 February 2013)

High throughput electrochemical techniques are widely applied in material discovery and optimization. For many applications, the most desirable electrochemical characterization requires a three-electrode cell under potentiostat control. In high throughput screening, a material library is explored by either employing an array of such cells, or rastering a single cell over the library. To attain this latter capability with unprecedented throughput, we have developed a highly integrated, compact scanning droplet cell that is optimized for rapid electrochemical and photoeletrochemical measurements. Using this cell, we screened a quaternary oxide library as (photo)electrocatalysts for the oxygen evolution (water splitting) reaction. High quality electrochemical measurements were carried out and key electrocatalytic properties were identified for each of 5456 samples with a throughput of 4 s per sample.
 [http://dx.doi.org/10.1063/1.4790419]

I. INTRODUCTION

Analysis of inorganic libraries is a powerful technique for materials discovery and optimization, as evident in the number and variety of recently published methods for combinatorial materials research.[1–3] A variety of parallel and serial scanning techniques has been implemented for combinatorial studies of (photo)electrocatalysts with varying compromises between throughput and quality of electrochemical data.[3–5] We present a scanning 3-electrode droplet cell that provides high quality electrochemical data and establishes a new throughput limit for scanning serial techniques. This instrument is designed for general (photo)electrochemical experiments and in this article, we highlight its use for the discovery of energy-related materials.

A potentiostat-controlled electrochemical cell is the standard tool for the measurement of electrochemical reactions. Parallel electrochemical methods typically replace the direct potentiostat measurement with a proxy for the reaction of interest by using pH imaging[6] or color imaging of fluorescent molecules[4,7] and organic dyes.[8,9] In addition to providing limited electrochemical information, these techniques function in a narrow pH range and are not suitable for highly acidic (pH = 0) or basic (pH = 14) environments. Traditional 2-electrode or 3-electrode photoelectrochemical cells incorporated with automated positioning systems[5,10,11] have the advantage of directly measuring the key electrochemical properties. However, the throughput of these reported techniques are limited either by the requirement of the custom designed substrate for electrical isolation of research samples, or the requirement for creating a liquid-tight seal for each sample. Scanning electrochemical microscopy (SECM)[12,13] is another scanning serial technique where a sensing electrode and/or a fiber optic tip is rastered across the material library to identify regions of high (photo)electrochemical activity. In the SECM screening, the entire material library is in contact with the electrolyte, permitting cross-contamination between neighboring compositions. The scanning droplet cell described in this article provides fast rastering capability and circumvents the common shortcomings of high throughput electrochemical techniques.

Scanning droplet cells and microcells refer to a variety of two- and three-electrode electrochemical cell designs in which capillary tubing delivers a small volume of electrolyte solution to a working electrode surface.[14,15] Initial microcells were developed for characterizing sub-200 μm heterogeneity in the electrochemical properties of surfaces, especially for corrosion studies.[16,17] Optimizing the cell design for spatial resolution, capillary cells with diameter as small as 10 μm diameter were developed and used to contact single crystallographic grains of a polished metal electrode.[18,19] The capabilities of such cells have also been expanded with the addition of light sources and downstream analytics for measuring reaction products.[20,21] A similar device with high spatial resolution has recently been incorporated in a probe station configuration and optimized for air-sensitive characterizations of thin films.[22] In essence, a composition library is a heterogeneous electrode whose properties can be mapped with a microcell, but the typical lateral sample dimension of 1 mm and the high premium placed on experiment throughput invoke new design principles. We enumerate the design criteria for high throughput library screening in the context of (photo)catalysis and present a cell design, which uniquely fulfills these criteria. The (photo)electrochemical performance of the cell is presented and the efficacy of this cell for high throughput screening is demonstrated by mapping the oxygen evolution electrocatalysis of a 5456-sample composition library. These high throughput experiments are integral to the discovery of new (photo)catalysts for solar-driven water-splitting.[5,23]

a)gregoire@caltech.edu.

II. EXPERIMENTAL

A. Cell design criteria

For high throughput (photo)electrochemical screening of composition libraries, the spatial resolution of the electrochemical cell must match the length scale for composition variations within the library. For continuous composition spreads, this length scale is the ratio of the desired composition resolution and the composition gradient. For discrete libraries, this length scale can be either the sample dimension or the sample pitch. In either case, this length scale is typically on the order of 1 mm and may be dictated by the resolution of material synthesis or chosen to match requirements of processing and measurement experiments.[23] The electrochemical experiment must also avoid the transport of sample material across this length scale as such contamination compromises the combinatorial experiment. Since elemental constituents may be amenable to dissolution during an electrochemical experiment, each sample should receive fresh solution.

The current density of interest can vary by many orders of magnitude depending on the application. For (photo)catalysis in energy-related applications, catalytic currents below 10 μA cm^{-2} are generally not of interest and some applications such as fuel cell catalysis require currents up to 1 A cm^{-2}. At the low current end, this requirement sets a limit for the electrochemical and electronic noise and sensitivity. At the high current end, the uncompensated resistance, i.e., the resistance from working to reference electrode, should be minimized to avoid undesirable voltage losses. The solution resistance between any pair of electrodes must be low enough to avoid issues with potentiostat compliance voltages.

With these requirements in place, cell design should be optimized for throughput. The cell must be capable of transitioning between samples rapidly and with vanishing failure rate. Upon arrival at a working electrode location, the settle time for stable solution contact to electrodes and stable solution flow should be minimized.

With these considerations, the critical design criteria can be succinctly listed: (1) incorporation of reference and counter electrodes with optimal configurations for low uncompensated resistance; (2) measurement of current densities from 10 μA cm^{-2} –1 A cm^{-2} during potentiostatic measurements using a standard commercial potentiostat; (3) 1 mm-scale spatial resolution on a planar working electrode; (4) efficient mass transport of reactants and products in both liquid phase and gas phase; (5) rapid movement between experiments and low settle time before starting an experiment; (6) mitigated sample cross-contamination from both dissolved and particulate species; (7) efficient integration of illumination sources for photoelectrochemical experiments.

B. High throughput scanning droplet cell design

We describe the design and function of a compact scanning droplet cell that can be used to attain solution contact to a planar working electrode with contact diameters varying from

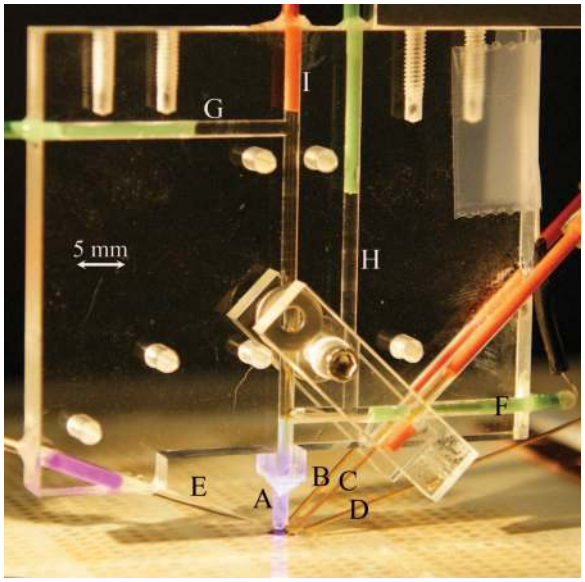

FIG. 1. A photograph of the scanning droplet cell suspended over a composition library. The drop of solution at the bottom of the cell contacts a 2.5 mm-diameter region of the working electrode containing a single 1 mm square sample. Nine ports (labeled A through I) are used for the solution flow and insertion of electrodes and fiber optic. The 385 nm light from an internal fiber optic illuminates the working electrode and produces a visible purple glow in the port A PTFE tube.

below 1 mm (0.0079 cm^2) to above 3 mm (0.28 cm^2). The cell shown in Fig. 1 was used for the (photo)electrochemical experiments described below and we provide the dimensions used to attain a 2.5 mm-diameter electrode contact. The droplet-forming tube at port A is fixed at a height of approximately 0.5 mm above the planar working electrode. Port A is terminated by tubing with inner and outer diameters of 1 mm and 1.55 mm, through which solution flows at a rate $R_A = 10$ μL/s. This solution influx is removed by ports B, C, and D, which are each terminated by the capillary tubing of inner and outer diameters of 0.2 mm and 0.38 mm, respectively. These ports are each pumped at a constant rate of approximately twice that of R_A. The excess pump rate results in suction of ambient gas into the ports. The port termination with the smallest radius from port A restricts the radius of the solution drop and thus defines the electrode contact area. When the cell moves with respect to the planar electrode in a direction away from the termination of port B, C, or D, the solution is efficiently removed by the respective trailing tube, with no visible solution drop left behind. With the three suction ports as arranged in Fig. 1, the cell can be rapidly rastered over a planar composition library.

This novel drop-restricting scheme circumvents the need for a gasket or a similar contact-based solution confinement mechanism. This property of the cell permits on-demand cell movement with no alteration to the solution flow and no vertical motion. The lateral accessibility of the solution droplet between the port A termination and the working electrode allows for the insertion of a capillary reference electrode at port E.

The counter electrode is introduced through the sealed port F and extends to the vertical channel that terminates at

port A. The cell can operate in two solution flow modes. The most direct scheme involves solution introduction at a rate R_A through port G. The solution then flows over the counter electrode and to port A. The counter electrode can also be differentially pumped by introducing solution at a rate $R_H > R_A$ into port H and pumping solution through port G at a rate R_H-R_A. This differential pumping mode has no effect on the solution drop at port A and flushes the counter electrode effluent to waste.

Port I is sealed and unused for electrochemical measurements. For photoelectrochemical experiments, an optical fiber is inserted in this bubble-free solution pathway and terminates in port A, which serves as a light guide for completing the optical path from the optical fiber to the working electrode. In Fig. 1, a 0.4 mm fiber optic is shown in this configuration, which facilitates illumination with any wavelength not strongly absorbed by the electrolyte.

The cell shown in Fig. 1 is made for compatibility with aqueous alkaline solutions. The housing is a 4.8 mm wide slab of plexiglass and all solution port terminations are either standard polyether ether ketone (PEEK) tubing or polytetrafluoroethylene (PTFE) tubing. For maximum droplet contact stability, the solution supply is provided by a syringe pump or gravity feed. Ports B, C, and D are continuously pumped by peristaltic pumps.

C. Combinatorial experiment

A quaternary metal-oxide library containing 5456 samples was screened for oxygen evolution electrocatalysis to demonstrate the throughput and reliability of the scanning droplet cell. The (Fe-Co-Ni-Ti)O_x thin-film catalyst library was deposited onto three glass plates coated with 400 nm of fluorine-doped tin oxide (FTO) according to previously reported ink-jet printing assisted cooperative-assembly methods.[24,25] Briefly, each Fe-Co-Ni-Ti composition in the library was synthesized by combining four "inks," each with an elemental precursor ($FeCl_3$, $Co(NO_3)_2 \bullet 6H_2O$, $Ni(NO_3)_2 \bullet 6H_2O$, and $TiCl_4$ obtained from Sigma Aldrich). Using vigorous stirring, 5 mmol of each metal precursor, 6 mmol of acid (HCl or HNO_3), and 0.5 g of F127 ($EO_{96}PO_{70}EO_{96}$, MW = 12000; Sigma Aldrich) were dissolved into 45 mL of ethanol. Using the inkjet printer (modified Epson Stylus Pro 4880), each composition sample was deposited onto a 1 mm^2 substrate area by dispensing a fixed volume of solution. The volumetric ratio of the inks was chosen to provide the desired metal stoichiometry, and each sample contained approximately 10 nmol of metal. The 5456 unique samples were deposited to cover the quaternary composition space with 3.33 at. % interval. The samples were evenly divided among the three glass plates and were processed with identical drying and precursor calcination steps. The as-deposited precursor library was then calcined at 350 °C for 5–6 h in a box furnace with flowing air. This calcination efficiently volatilized and removed the precursor ligands and other ink components, and additionally yielded oxidation of the metals. The resulting samples were non-contiguous metal oxide coatings with each sample well adhered to the FTO coating and contained within the designed 1 mm^2 electrode area. The grid of samples on each plate shared the common FTO contact layer.

High throughput electrochemical and photoelectrochemical experiments were performed on each library using the cell shown in Fig. 1 and a Gamry G 300 potentiostat controlled with custom automation software. The 3-electrode cell was outfit with a Pt wire counter electrode and custom made Ag/AgCl reference electrode. The capillary reference electrode was pulled from 1 mm outer diameter, 0.5 mm inner diameter glass tube and then broken as a micro-injection needle, yielding a tip with approximate inner and outer diameters of 25 and 75 μm. Using this capillary and a 0.2 mm Ag wire, a Ag/AgCl reference electrode was synthesized by standard techniques and calibrated to a commercial electrode before and after electrochemical experiments.

A standard 2-axis translation stage was used to raster the library below the fixed droplet cell with an average speed of approximately 2.5 mm s^{-1} over the 2 mm sample pitch. Cyclic Voltammetry (CV) was performed on each sample. After approximately 0.8 s of translation to the sample, the working electrode was held at the starting potential of the CV for 2 s. A settle time of at least 1 s was needed to stabilize the droplet volume and electrode contact, and the total 2 s duration was used to additionally stabilize the electrode at this potential and mitigate electrochemical transients at the beginning of the CV measurement. To screen the library samples for electrocatalysts (EC) of the oxygen evolution reaction (OER), the CV measurement was performed from –0.09 V to 0.51 V with respect to the O_2/H_2O Nernst potential in the aqueous electrolyte solution of O_2-bubbled 0.1 M NaOH. At a scan rate of 1 V s^{-1}, this voltage range was covered on both the forward and reverse legs of the single cycle CV measurement for a total experiment time of 1.2 s and a sample throughput of one sample every 4 s.

The composition library was also scanned for OER photoelectrocatalysis (PEC) in a similar manner. After sample-cell positioning, open circuit was maintained for 2 s followed by a chronoamperometric measurement in which the sample was held at the O_2/H_2O equilibrium potential and the sample was illuminated with a 2 Hz square wave profile alternating between no illumination and 2.5 mW from a 385 nm light emitting diode (LED). The incident power on the working electrode was measured before the high throughput experiment using a transparent quartz plate contacted by the droplet cell with a standard power meter pressed against the other side of the plate in transmission geometry. Chopped-illumination CVs and other electrochemical techniques can similarly be performed, but the throughput is limited by the equilibration time of the measured current after toggled illumination, which is approximately 0.25 s for these samples. While in principle this photoelectrochemical experiment can be performed in 1 s so that the 4 s per sample throughput can be attained, a 6.5 s experiment containing 6 illumination pulses was used in this study to demonstrate the stability of the photocurrent measurement. A variety of electrochemical and photoelectrochemical experiments can also be performed on each sample to avoid the duplication of the motion and settle time.

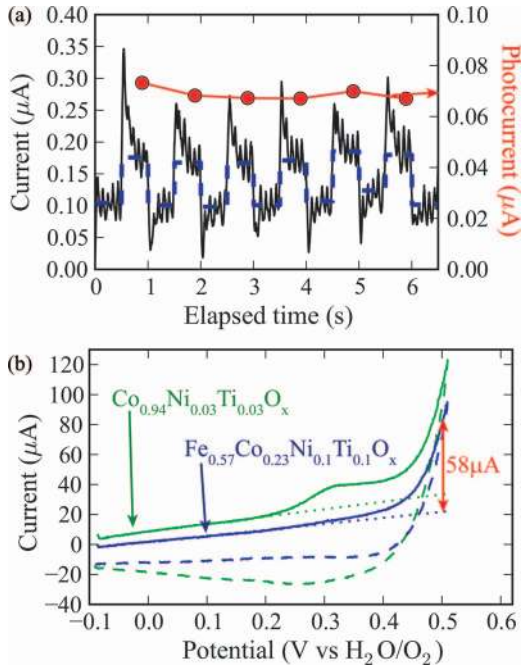

FIG. 2. (a) The photoelectrochemical characterization of a $Fe_{0.6}Co_{0.26}Ni_{0.07}Ti_{0.07}O_x$ sample in 0.1 M NaOH. The current (black) at a fixed potential was measured during 2 Hz cycling of illumination. The measured current after each illumination transition (blue, dashed) was analyzed and indicated a 70 nA photocurrent (red, right vertical axis). (b) CVs for characterization of a $Fe_{0.57}Co_{0.23}Ni_{0.1}Ti_{0.1}O_x$ (blue) and a $Co_{0.94}Ni_{0.03}Ti_{0.03}O_x$ (green) sample for OER electrocatalysis in 0.1 M NaOH. The forward (solid) and reverse (dashed) sweeps are shown along with the residual current for the forward sweep (dotted). The FOM of catalytic current at 0.5 V is labeled on the blue trace.

III. RESULTS AND DISCUSSION

A. (Photo)electrochemical results

Figure 2 shows example electrochemical data from the PEC and EC experiments described above. The PEC data of Fig. 2(a) shows the measured current at fixed potential as the ultraviolet illumination is chopped. Visual inspection of the measured current reveals 10 Hz sinusoidal noise, the source of which is under investigation. The data clearly show higher anodic current during illumination. After the approximately 0.25 s transient, the average current for each illuminated and dark segment was calculated. The photocurrent was calculated as the difference between illuminated current and the average neighboring dark currents. For the 6 illumination cycles, the measured photocurrent for the 1 mm^2 electrode was 70 ± 3 nA. While this sample is not a noteworthy photocatalyst, this result demonstrates sub-10 $\mu A\ cm^{-2}$ photocurrent detection, as required by criterion 2.

Figure 2(b) contains two typical CV scans in the quaternary library provided by the droplet cell. Both forward traces contain residue current from capacitive charging through the series resistance in the system and an exponentially increasing current indicative of OER catalysis. Additionally, the green trace shows clear redox activity of the sample material near 0.3 V vs. the Nernst potential of OER in the solution. For each CV, the forward sweep was processed by automatically calculating and subtracting the linear residual current. At a given overpotential, the catalytic current was measured as the difference between the forward sweep anodic current and the modeled residual current. We used the current at 0.5 V overpotential as a figure of merit (FOM) for OER electrocatalyst screening. For the sample of Fig. 2(b), the figure of merit of 58 μA is labeled, which for this 1 mm^2 of planar electrode area corresponds to a current density of 5.8 mA cm^{-2}. Similar analysis was performed for every sample in the library.

For one of the three plates containing the (Fe-Co-Ni-Ti)O_x library, Fig. 3(a) shows an optical image while Fig. 3(b) shows the FOM map. Combined with the corresponding data for the additional two plates, the FOM composition map is constructed and displayed in Figs. 3(c) and 3(d). The former contains a 2-d projection of the quaternary composition space, which is not sufficient for identification of the quaternary composition trends. To facilitate this visual analysis, Fig. 3(d) contains a series of ternary composition plots, each a flattened slab from Fig. 3(c) of thickness 10 at. % Ti. These plots show that appreciable current is attained in a wide composition range surrounding the 3-metal composition $(Fe_{0.2}Co_{0.2}Ni_{0.6})O_x$ and that the ternary region of high FOM narrows with increasing Ti content up to 40 at. % Ti. At all higher concentrations of Ti, the FOM is quite low, which is expected given the very low catalytic current of titanium oxides. At 0.5 V overpotential, the FTO coating yields a small background current, which is comparable to the lowest FOM value in these figures.

The repeatability of electrochemical characterizations with this scanning droplet cell was verified by several methods and here we show the results for repeated mapping of the ternary (Fe-Ni-Co)O_x compositions in the library. Fig. 4 shows the resulting FOM maps for 3 separate raster scans of the ternary library and demonstrates that the FOM value and composition trend was well reproduced for the majority of the composition range. The FOM for the Ni-rich region increased with repeated testing, which we assert is due to evolution of these catalysts.

B. Cell performance

For the (photo)electrochemical experiments highlighted in Figs. 2–4, the scanning droplet cell meets each of the established design criteria. The droplet volume is flushed approximately once per second, which is sufficient for the mass transport of reactants and products. Upon the completion of electrochemistry on a given sample, the droplet volume is completely captured by the lagging suction port during sample movement, which precludes sample cross-contamination by dissolved species. During sample motion, consistent solution contact with the planar electrode is maintained by continuing the pumping schedule, but it is worth noting that contact with the working electrode can be severed through interruption of the solution flow into port A during cell movement. We also note that static solution experiments are easily performed by ceasing solution flow into port A at a fixed cell position, which results in a sub-1 s transient during which the removal of solution at the perimeter of the droplet results in a pinching off of the droplet such that it is no longer in contact with

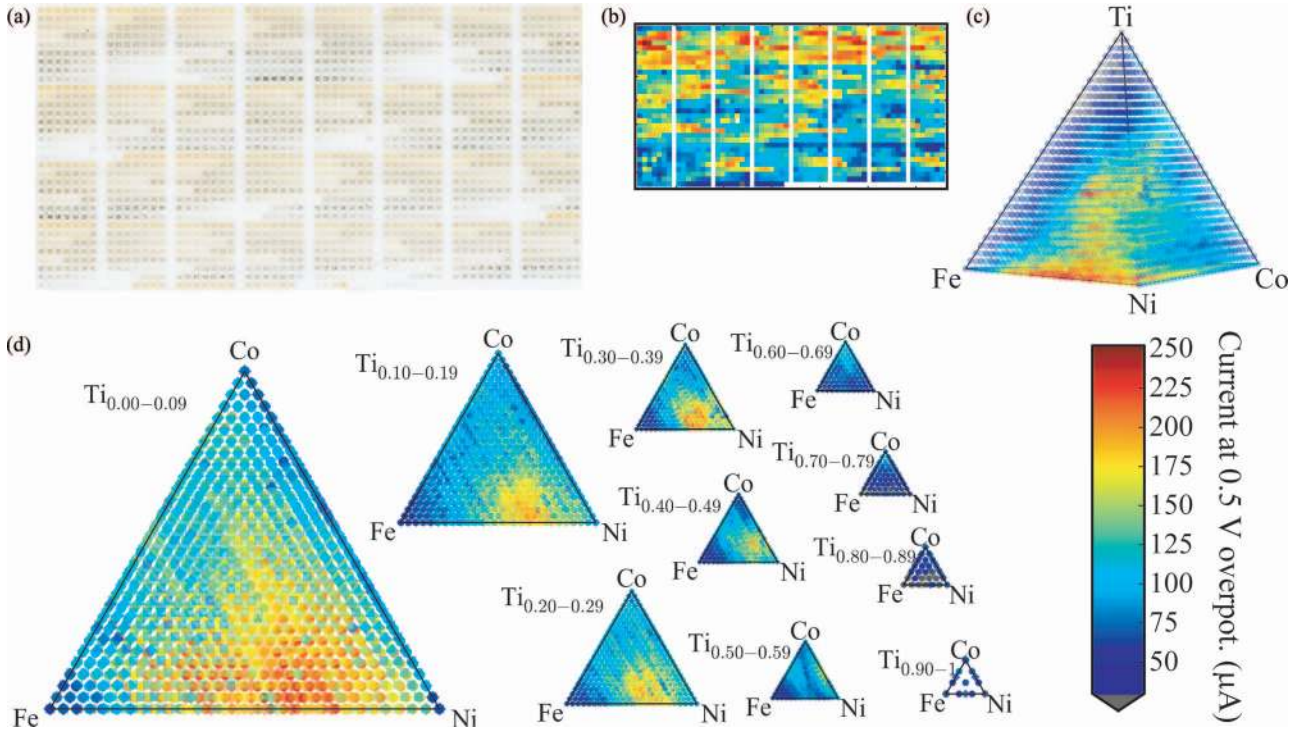

FIG. 3. Mapping of the OER catalytic current at 0.5 V overpotential in 0.1 M NaOH. This FOM for each sample of a metal oxide composition library plate (photograph in (a)) is shown in (b) using the false color scale at the bottom right. Combined with two additional plates, the quaternary composition map is shown in (c), where the horizontal planes of data points correspond to 3.3 at. % intervals of Ti concentration. Sets of three planes are plotted together in each of 10 ternary composition plots shown in (d).

the suction ports. The resulting static droplet makes contact to a slightly smaller and highly reproducible working electrode area.

For different screening applications, the scan rate in the CV measurements can be adjusted to facilitate the throughput of the screening without compromising (photo)electrochemical data quality. For screening (photo)electrocatalysis of solar-driven water-splitting reactions, the relevant catalytic current density is on the order of 10 mA cm^{-2} at an overpotential no more than 0.5 V.[23] In the study discussed above, the CV parameters were chosen to cover the applicable range of overpotential while keeping the measurement duration (1.2 s) from creating a bottleneck in the screening process. Chronopotentiometry and chronoamperometry measurements were also applied in this study to identify material compositions with high electrocatalytic activity for OER reactions and similar FOM trends were observed using these techniques. The high speed for the CV measurements as well as the rich information contained in the current vs. voltage characteristics were considered to be a superior screening technique for this application and material system.

Miniaturization of an electrochemical cell often leads to a large uncompensated resistance R_u between working and reference electrode, yielding undesirably large IR_u potential drops. In the configuration described above, the uncompensated resistance is approximately $R_u = \sigma^{-1} \times 2.7\ cm^{-1}$, where σ is the solution conductance. The electrochemical data in Figs. 2–4 were collected using a low conductivity solution of $\sigma = 18$ mS cm^{-1}, but the IR_u loss of less than 0.1 V does not significantly impact the FOM trend. By using a solution with a more appreciable conductance of $\sigma = 180$ mS cm^{-1} (1 M NaOH), the uncompensated resistance is approximately 15 Ω. With the 1 mm^2 samples and the

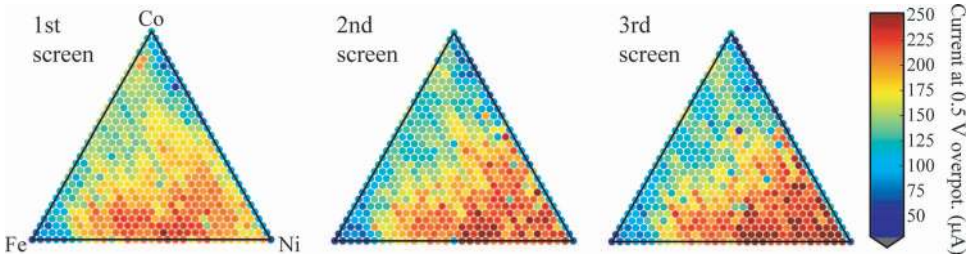

FIG. 4. The mapping shown in Fig. 3 is repeated by rastering the droplet cell over the (Fe-Co-Ni)O_x ternary compositions in three separate screens. The results from each of the three screenings demonstrated that the FOM is well repeated for most compositions but increases with repeated testing for Ni-rich compositions due to an aging phenomenon of Ni-rich electrocatalysts.

targeted solar-driven water-splitting current density (10 mA cm^{-2}), the IR_u loss is less than 2 mV. This negligible loss circumvents the need for IR_u compensation corrections and highlights the utility of the scanning droplet cell.

The solution impedance between working and counter electrodes of the cell design discussed above supports approximately 0.3 A cm^{-2} with $\sigma = 180$ mS cm^{-1}, assuming a 10 V potentiostat compliance. While higher current densities are not of interest for our solar water splitting application, criterion 2 was established for broad applicability of this cell design. While current densities up to 1 A cm^{-2} can be supported through an increase in solution conductance or larger compliance voltage, we note that the geometric resistance can be reduced by at least a factor of 4 by increasing the inner tube diameter of port A, shortening the port A tube, and lowering the position of port F. These modifications are preferable to placing the counter electrode in the port A tube, which would yield very low geometric resistance, because this design modification compromises criterion 4 and blocks the fiber optic access.

Given these electrochemical capabilities, the primary throughput metric for scanning serial measurements is the time between the end of the experiment on one sample and the beginning of the experiment on the next. A cell design that uses a gasket to provide a solution-tight seal requires solution removal, vertical motion before and after lateral movement to the next sample, and solution filling. By avoiding these time consuming steps, the scanning droplet cell attains an unprecedented experiment throughput for (photo)electrochemical measurements with a 3-electrode cell.

For cost-effective high throughput synthesis, the conductive layer on the plate is not patterned, resulting in a common working electrode for the grid of samples. If groups of isolated contacts exist on the library, increased measurement throughput can be attained with parallel measurements. That is, an array of electrochemical cells can easily be constructed by laterally stacking duplicates of the slab construction shown in Fig. 1, provided that the working electrode of each cell is electrically isolated.

IV. SUMMARY

We present a scanning droplet cell optimized for scanning-serial mapping of the (photo)electrochemical properties of a composition library. The cell is suspended at a controlled distance above the working electrode and a carefully engineered flow pattern of the electrolyte solution provides solution contact to a well-defined working electrode area. This unique construction permits rapid rastering of the cell over a planar working electrode, a capability that enables increased experiment throughput for combinatorial (photo)electrochemical studies. The sensitivity of the cell to sub-10 μA cm^{-2} photocurrent was demonstrated in a chronoamperometric experiment with chopped illumination. The high throughput operation of the cell was demonstrated by performing a 0.6 V, full-cycle CV measurement at a throughput of one sample every 4 s. With this latter experiment, a $(Fe\text{-}Co\text{-}Ni\text{-}Ti)O_x$ quaternary composition space with 5456 samples was mapped for OER electrocatalysis.

ACKNOWLEDGMENTS

This material is based upon work performed by the Joint Center for Artificial Photosynthesis, a DOE Energy Innovation Hub, supported through the Office of Science of the U.S. Department of Energy (Award No. DE-SC0004993). The authors thank Mr. Lung-Sheng Lin for assistance in fabrication of the cell and Mr. William Fisher of Lawrence Berkeley National Laboratory for assistance in fabrication of the capillary for the reference electrode. The authors also thank Dr. Eric McFarland, Dr. Nathan Lewis, Dr. Carl Koval, and Dr. Joachim Lewerenz for helpful discussions.

[1]Z. H. Barber and M. G. Blamire, Mater. Sci. Technol. **24**, 757 (2008).
[2]R. Potyrailo, K. Rajan, K. Stoewe, I. Takeuchi, B. Chisholm, and H. Lam, ACS Comb. Sci. **13**, 579 (2011).
[3]T. H. Muster, A. Trinchi, T. A. Markley, D. Lau, P. Martin, A. Bradbury, A. Bendavid, and S. Dligatch, Electrochim. Acta **56**, 9679 (2011).
[4]E. Reddington, A. Sapienza, B. Gurau, R. Viswanathan, S. Sarangapani, E. Smotkin, and T. Mallouk, Science **280**, 1735 (1998).
[5]M. Woodhouse and B. A. Parkinson, Chem. Soc. Rev. **38**, 197 (2009).
[6]A. Nakayama, E. Suzuki, and T. Ohmori, Appl. Surf. Sci. **189**, 260 (2002).
[7]J. B. Gerken, J. Y. C. Chen, R. C. Massé, A. B. Powell, and S. S. Stahl, Angew. Chem. **51**, 6676 (2012).
[8]J. Ding, J. Bao, S. Sun, Z. Luo, and C. Gao, J. Comb. Chem. **11**, 523 (2009).
[9]A. Kafizas, D. Adriaens, A. Mills, and I. P. Parkin, Phys. Chem. Chem. Phys. **11**, 8367 (2009).
[10]T. F. Jaramillo, S.-H. Baeck, A. Kleiman-Shwarsctein, K.-S. Choi, G. D. Stucky, and E. W. McFarland, J. Comb. Chem. **7**, 264 (2005).
[11]J. E. Katz, T. R. Gingrich, E. A. Santori, and N. S. Lewis, Energy Environ. Sci. **2**, 103 (2009).
[12]S. P. Berglund, A. J. E. Rettie, S. Hoang, and C. B. Mullins, Phys. Chem. Chem. Phys. **14**, 7065 (2012).
[13]J. S. Jang, J. Lee, H. Ye, F. F. Fan, and A. J. Bard, J. Phys. Chem. C **113**, 6719 (2009).
[14]J. W. Schultze and A. Bressel, Electrochim. Acta **47**, 3 (2001).
[15]M. M. Lohrengel and A. Moehring, in *Electrochemical Microsystem Technologies*, edited by J. W. Schultze, T. Osaka, and M. Datta (Taylor & Francis, Andover, 2002).
[16]M. M. Lohrengel, A. Moehring, and M. Pilaski, Electrochim. Acta **47**, 137 (2001).
[17]T. Suter and H. Bohni, Electrochim. Acta **42**, 3275 (1997).
[18]A. W. Hassel and M. Seo, Electrochim. Acta **44**, 3769 (1999).
[19]M. Lohrengel, S. Heiroth, K. Kluger, M. Pilaski, and B. Walther, Electrochim. Acta **51**, 1431 (2006).
[20]A. W. Hassel and M. Seo, Electrochem. Soc. Proc. **99–27**, 337 (1999).
[21]M. Voith, G. Luckeneder, and A. W. Hassel, J. Solid State Electrochem. **16**, 3473 (2012).
[22]L. Small, A. Cook, C. Apblett, J. F. Ihlefeld, G. Brennecka, and D. Duquette, J. Electrochem. Soc. **159**, F87 (2012).
[23]M. G. Walter, E. L. Warren, J. R. McKone, S. W. Boettcher, Q. Mi, E. A. Santori, and N. S. Lewis, Chem. Rev. **110**, 6446 (2010).
[24]J. Fan, S. W. Boettcher, and G. D. Stucky, Chem. Mater. **18**, 6391 (2006).
[25]X. Liu, Y. Shen, R. Yang, S. Zou, X. Ji, L. Shi, Y. Zhang, D. Liu, L. Xiao, X. Zheng, S. Li, J. Fan, and G. D. Stucky, Nano Lett. **12**, 5733 (2012).